Acc. Chem. Res. **1998,** *31,* 474−484

Synthetic Strategies, Structure Patterns, and Emerging Properties in the Chemistry of Modular Porous Solids†

OMAR M. YAGHI,* HAILIAN LI, CHARLES DAVIS, DAVID RICHARDSON, AND THOMAS L. GROY

Department of Chemistry and Biochemistry, Goldwater Center for Science and Engineering, Arizona State University, Box 871604, Tempe, Arizona 85287-1604

Received December 4, 1997

Background

The designed construction of extended porous frameworks from soluble molecular building blocks represents one of the most challenging issues facing synthetic chemistry today. Recently, intense research activities directed toward the development of this field have included the assembly of inorganic metal clusters,[1] coordination complexes,[2] and organic molecules[3] of great diversity into extended motifs that are held together either by strong metal−ligand bonding or by weaker bonding forces such as hydrogen-bonding and $\pi-\pi$ interactions. Materials that have been produced in this way are referred to as *modular* since they are assembled from discrete molecules which can be modified to have well-defined function.[4] The fact that the integrity of the building blocks is preserved during the synthesis and ultimately translated into the resulting assembled network offers numerous opportunities for designing frameworks with desirable topologies and architectures, thus paving the way for establishing connections between molecular and solid properties. At least three challenges have emerged in this area that must be reckoned with in order for the ideas of rational and designed synthesis of porous materials to become a reality with routine utility. First, it is difficult to control the orientation and stereochemistry of the building blocks in the solid state in order to achieve a given target molecular topology and architecture. Second, in most cases, the products of such assembly reactions are obtained as poorly crystalline or amorphous solids, thus prohibiting their full characterization by single-crystal X-ray diffraction techniques. Third, access to the pores within open structures—an aspect that is so critical to their utility as porous materials—is often prevented by either self-interpenetration as observed for very open frameworks or strong host−guest interactions that lead to the destruction of the host framework when removal or exchange of guests is attempted.

To define and investigate the parameters contributing to the assembly of materials from molecular building blocks, we have established a program aimed at constructing modular porous networks by linking inorganic metal sulfide clusters and organic molecules with transition metal ions. Our work has focused primarily on studying the issues outlined above, and this Account presents our progress toward finding viable and general solutions to these challenges. This is illustrated by some representative examples chosen from the chemistry developed in our research effort for the three building blocks shown in **a**−**c**. Their functionality, shape, size, and reactivity provide insight into materials design and its utility in producing anionic, cationic, and neutral porous frameworks. Specifically, this contribution outlines (1)

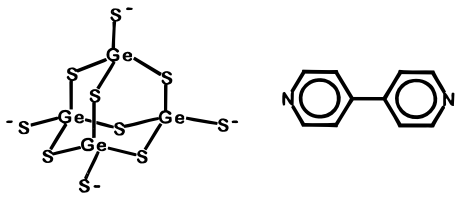

a **b** **c**

Omar M. Yaghi was born in Jordan (1965). He received his B.S. degree in chemistry from the State University of New York—Albany (1985) and his Ph.D. from the University of Illinois—Urbana (1990) with Professor Walter G. Klemperer. From 1990 to 1992, he was an NSF Postdoctoral Fellow at Harvard University with Professor Richard H. Holm. He joined the faculty at Arizona State University in 1992. Currently he is an Associate Professor of Chemistry, establishing several research programs dealing with the transformation of molecular organic and inorganic building blocks into functional extended frameworks.

Hailian Li was born in Jiangsu, China, in 1964. He received his B.S. (1987) and M.S. (1990) degrees in chemistry from Nanjing University, China. He is currently a Faculty Research Associate with Professor O. M. Yaghi at Arizona State University. His primary focus is on the synthesis of porous crystalline materials with novel linkages.

Charles Davis was born in Nuremberg, Bavaria, Germany, in 1966. He received his B.S. degree in chemistry from Louisiana State University in Shreveport in 1993. Currently, he is completing his Ph.D. in inorganic chemistry at Arizona State University. His graduate work has focused on understanding the inclusion chemistry of metal−organic microporous solids.

David Richardson was born in Dayton, OH in 1960. He holds a B.S. degree in biology (1982) and B.S. (1984), M.S. (1989), and Ph.D. (1991) degrees in chemistry from Arizona State University. Currently, he is performing postdoctoral work in non-oxide porous materials.

Thomas L. Groy was born in Colorado in 1954. He received his Ph.D. with Sheng H. Lin at Arizona State University in 1982, developing theory on the scattering of electrons and X-rays from small crystalline particles. He is currently an Associate Research Professional, specializing in X-ray structural analysis for the Department of Chemistry and Biochemistry at Arizona State University.

* Phone: (602) 965-0057. Fax: (602) 965-2747. E-mail: oyaghi@asu.edu.

† Dedicated to Professor Richard H. Holm on the occasion of his 65th birthday.

S0001-4842(97)00151-9 CCC: $15.00
Published on Web 07/01/1998

Scheme 1

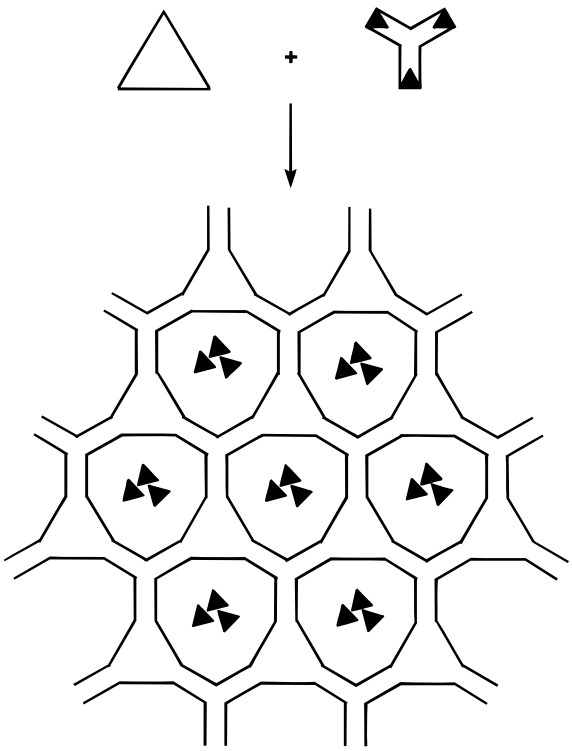

various synthetic strategies developed for producing porous modular networks in *crystalline* form using diffusion, solvothermal, and gel crystal growth techniques, (2) methods of achieving rigid, noninterpenetrated, and truly porous modular frameworks capable of reversible binding and removal of guests without affecting the structural integrity of the host framework, and (3) emerging novel properties and prospective applications resulting from tailoring the molecular building blocks and the metal ion centers of the host structure.

General Strategies for the Construction of Porous Modular Solids

Condensation−addition polymerization reactions have been utilized for the preparation of porous materials from organic molecules, metal clusters, and transition metal ions. This is illustrated in Scheme 1 for a hypothetical 2-D porous structure resulting from the addition of a well-characterized and distinct molecular building block (triangle) to a trigonal planar metal complex (Y-shaped). Loss of the ligands or counterions (small triangles), which are associated with the metal ion, allows for their incorporation into the pores as molecular or ionic guests depending on the framework charge. In this way, the intrinsic bonding geometry of the metal ion linker along with the functionality of the building blocks direct the assembly into a porous framework that is held together by coordination bonds. In principle, a limitless number of possibilities exist for exploiting the metal ion environment and the size and functionality of the building blocks toward producing tailored pores of diverse sizes, shapes, and functions.

Decorated Diamond Nets: Porous Metal Sulfide Materials

Generally, the assembly reaction described above yields extended open frameworks that can be related to basic inorganic nets. For example, diffusion of an aqueous solution of $Mn(CH_3CO_2)_2 \cdot 4H_2O$ into another aqueous solution of $Ge_4S_{10}[(CH_3)_4N]_4$ gives yellow crystals of $MnGe_4S_{10} \cdot 2(CH_3)_4N$.[1d] The structure of this compound (Figure 1) can be understood in terms of the diamond net, where the C vertexes have been alternately replaced by $Ge_4S_{10}^{4-}$ cages, **a**, and tetrahedral Mn(II) centers. The C−C bonds are then replaced by doubly bridging S^{2-}, to yield a framework that may be referred to as a decorated diamond net.[5,6] However, unlike diamond, the decorated net is porous due to the larger size of the inorganic cages compared to carbon atoms. We found that the pores are occupied with tetramethylammonium cations, which can be thermally decomposed without destruction of the metal sulfide $MnGe_4S_{10}^{4-}$ framework. The Mn−Ge−S framework is stable up to 500 °C under inert atmosphere. The tetramethylammonium ions are exchangeable with Cu^{2+}, Ni^{2+}, Zn^{2+}, Hg^{2+} and Cd^{2+} as determined by infrared spectroscopy along with X-ray powder diffraction.[1d,7]

The successful synthesis of this compound and its structural characterization by single-crystal X-ray diffraction pointed to the viability of using the building block approach for the synthesis of new classes of crystalline porous materials; it provided the first fully characterized 3-D porous metal sulfide in an area that had just emerged,[8a] and continues to expand.[8b−e] The available opportunities for establishing variation on this theme using hybrid organic/inorganic networks have also been pursued by our group as outlined below.

Porous Metal 4,4′-Bipyridine Cationic Frameworks

At the outset of this work, cationic frameworks were unknown in the literature of crystalline porous materials; however, recent work in modular chemistry has allowed the assembly of 3-D extended cationic frameworks. We and others have prepared a diverse class of cationic open networks by reacting simple metal ion salts with neutral building blocks such as, 4,4′-bipyridine (BPY), **b**, to yield structures having nets analogous to those of diamond[7,9] and α-$ThSi_2$,[10] and others that have topologies related to hexagonal,[11] square grids,[2a,b,e,h,k] railroad,[12] and ladder motifs[2b] as shown in Figure 2.

Cationic Porous Networks and Anion Exchange. A cationic diamond-like network was synthesized by the combination of acetonitrile solutions of $Cu(CH_3CN)_4PF_6$ and BPY at room temperature, which gives orange crystals of $Cu(BPY)_2 \cdot PF_6$ in high yield.[7,9a] The crystal structure of this compound reveals the presence of four interpenetrated diamond-like $Cu(BPY)^+$ frameworks with tetrahedral Cu(I) linking together rod-like BPY building blocks to form a tetragonal lattice with the PF_6 anions occupying a 3-D channel system of nearly 7 Å aperture, as shown in Figures 2a and 3a. Examination of the channels reveals

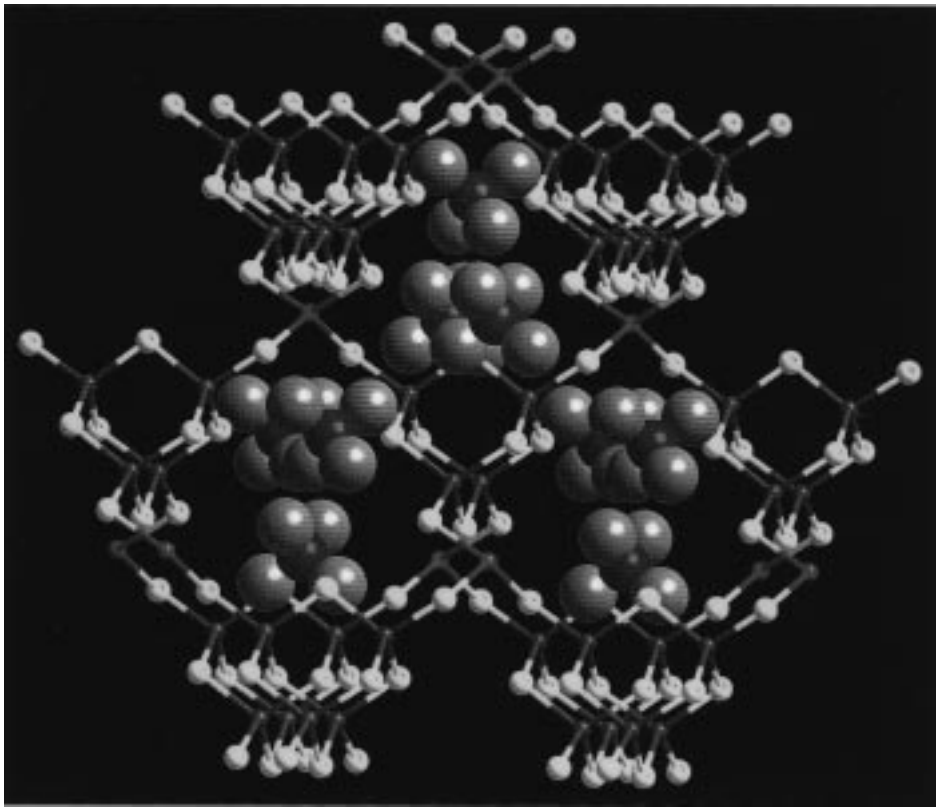

FIGURE 1. Crystal structure of $MnGe_4S_{10}\cdot 2(CH_3)_4N$, where the 3-D extended porous system of the diamond-like $MnGe_4S_{10}^{2-}$ framework (Mn, red; Ge, blue; S, yellow) is occupied with the tetramethylammonium cations (N, large green; C, large gray). The hydrogen atoms of the cations have been omitted for clarity.

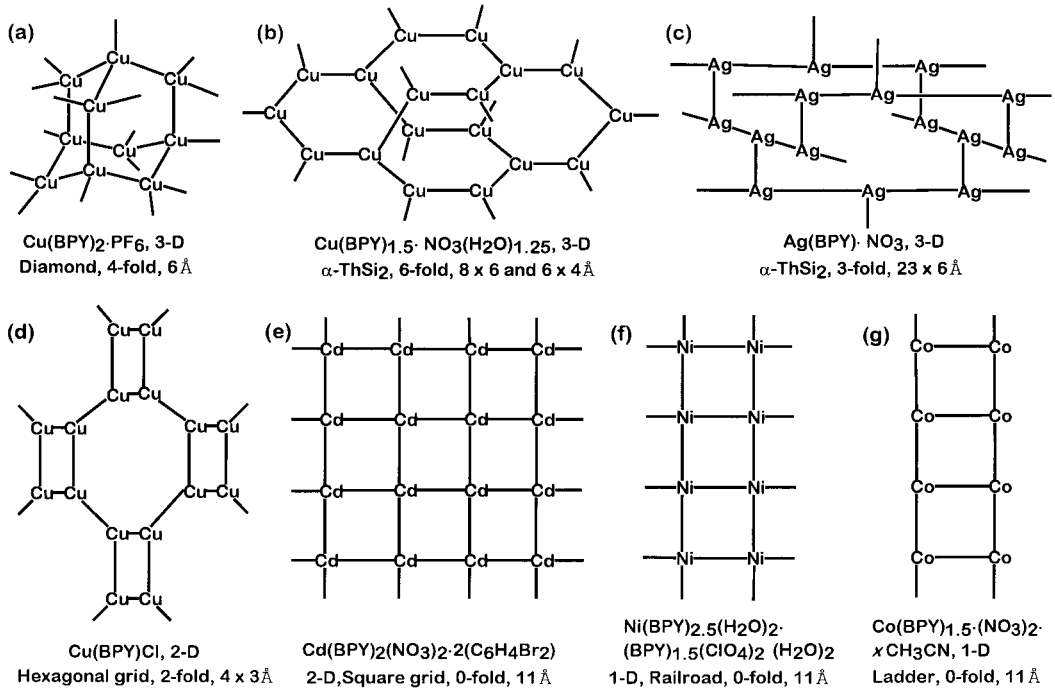

FIGURE 2. Line representations of typical metal 4,4′-bipyridine (M−BPY) porous extended networks, where the lines represent BPY [except the vertical lines in (c) and the horizontal lines in (d), respectively indicate Ag−Ag and Cu−Cu]. The chemical formula, dimensionality of the M−BPY framework, structure type, number of interpenetrating frameworks, and pore aperture are listed respectively beneath each representation.

that they are generated by four Cu−BPY strands from independent frameworks, which give the channels an overall helical conformation as shown in Figure 3b. It appears that the host−guest ionic interactions are of sufficient strength to prevent ion exchange, as attempts to introduce other inorganic anions such as BF_4^-, CN^-,

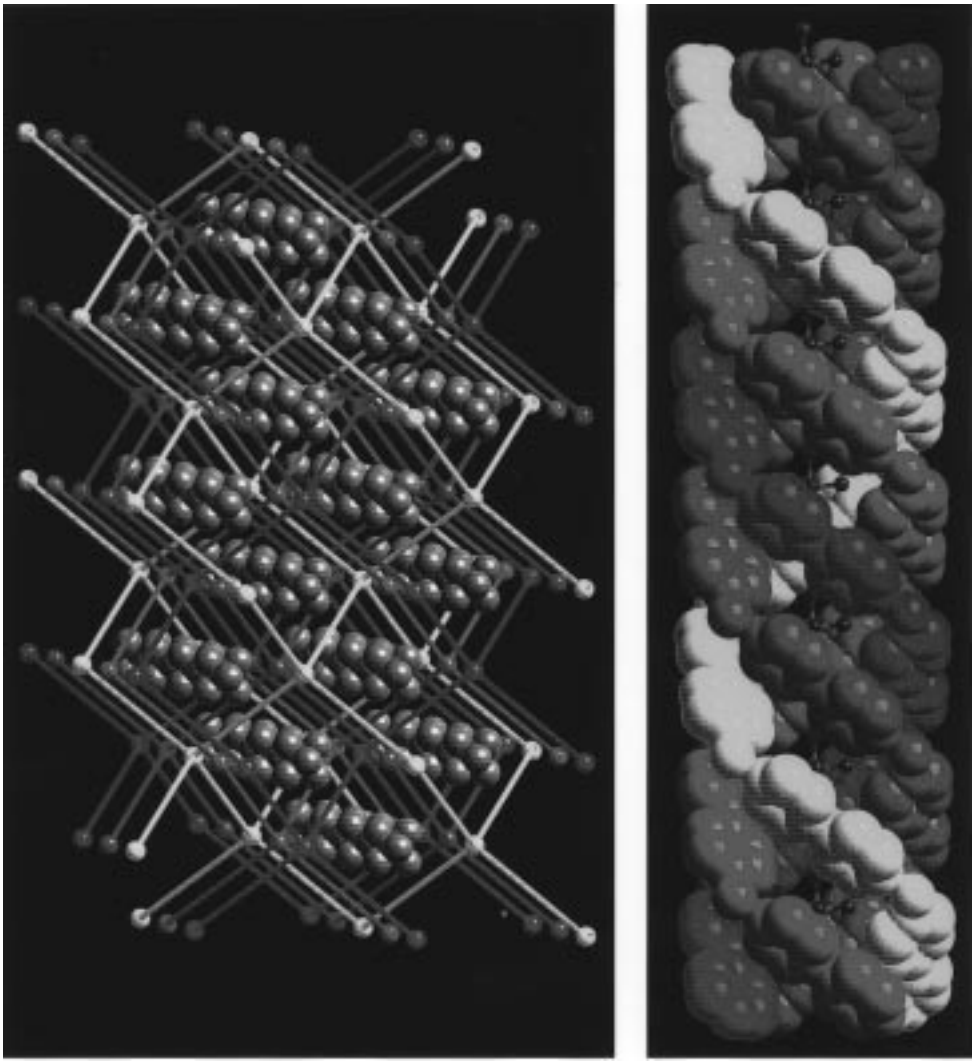

FIGURE 3. (a, left) The four interpenetrated diamond-like $Cu(BPY)^+$ networks (each drawn with a different color) in the crystal of $Cu(BPY)_2 \cdot PF_6$, with Cu and BPY represented as a sphere and rod, respectively. The remaining pore space is filled with PF_6 anions (P, large magenta spheres; F, large gray spheres). (b, right) A view showing the helical nature of the $Cu(BPY)^+$ chains (drawn in space-filling representation), which yield the channels where the PF_6^- (P, magenta; F, green spheres) resides.

and MoO_4^{2-} resulted in the formation of condensed and nonporous phases.

By using hydrogen-bonded aggregates as guests, it was possible to successfully perform anion exchange on the compound $Cu(BPY)_{1.5} \cdot NO_3(H_2O)_{1.25}$.[10a] Here, nitrate–water hydrogen-bonded aggregates reside in 8 × 6 and 4 × 6 Å channels, which are supported by six identical interpenetrated $Cu(BPY)_{1.5}^+$ frameworks, having Cu(I) linked to three BPY in a trigonal planar conformation to yield a network analogous to that of the Si net in α-$ThSi_2$ as shown in Figures 2b and 4. By thermally liberating the water guests, it was possible to enhance the lability of the nitrate guests and allow their exchange with anions such as SO_4^{2-} and BF_4^-.

The geometry at the metal center has tremendous impact on the pore architecture as well as its function. This is evident in the compound $Ag(BPY) \cdot NO_3$, where $Ag(BPY)^+$ chains are cross-linked through Ag–Ag bonds (2.977(1) Å) to form a 3-D porous framework with large rectangular channels of 23 × 6 Å dimension, as shown in Figures 2c and 5.[10b] This void space exists despite the presence of three interpenetrated frameworks. The topology of a single framework in this structure is analogous to that of the Si net in α-$ThSi_2$.

The T-shaped coordination of silver leaves an open coordination site in a trans position to the Ag–Ag bonds, pointing toward the center of the channels, where the nitrate guests form very weak interactions with silver (Ag–O = 2.78(1) Å). Initial evaluation of the ion-exchange properties of this material reveals that the nitrate can be exchanged with PF_6^-, BF_4^-, SO_4^{2-}, and MoO_4^{2-} without destruction of the framework, as determined by infrared spectroscopy, elemental microanalysis, X-ray powder diffraction, and optical microscopy. The experimental procedure of a typical example involving ion exchange with PF_6^- is outlined here: A slight excess of $NaPF_6$(aq) was added to a suspension of microcrystalline Ag(4,4′-bpy)·NO_3 in water at room temperature and allowed to stand for 6 h, then filtered, and washed with several aliquots of water and diethyl ether, followed by air-drying. The FT-IR spectra of the original and the exchanged solid are shown, respectively, in Figure 6a,b. Here, intense PF_6^-

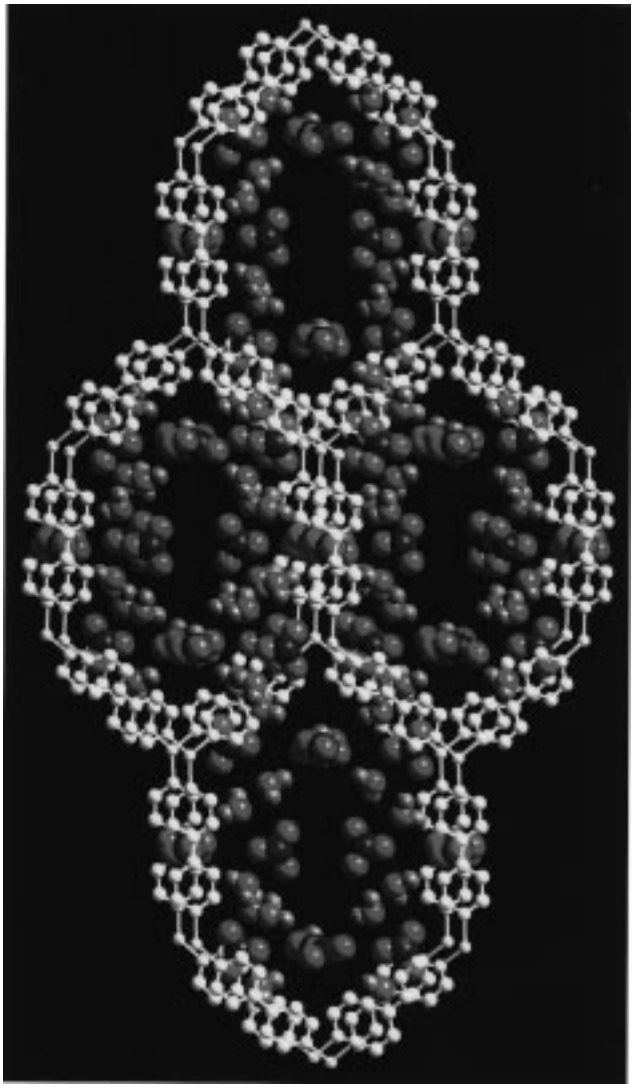

FIGURE 4. A view of a single $Cu(BPY)^{+}$ network (yellow) in the 6-fold interpenetrated structure of $Cu(BPY)_{1.5}{\cdot}NO_3(H_2O)_{1.25}$, where hydrogen-bonded aggregate guests (N, green; O, red; H, gray) have been utilized to fill the large pore space remaining in the crystal. The hydrogen atoms on BPY have been omitted for clarity.

bands at 835 and 564 cm^{-1} begin to appear as intense NO_3^- bands from 1385 to 1335 cm^{-1} disappear, with the rest of the spectrum remaining virtually unchanged. As KNO_3(aq) is added to the exchanged material, the PF_6^- bands disappear while the NO_3^- bands reappear to yield the original material as shown in Figure 6c. To examine the stability of this framework during the ion-exchange process, we monitored the material by X-ray powder diffraction (XRPD) as shown in Figure 6d−f. Colorless transparent crystals of the unexchanged material become opaque upon complete exchange; however, they still give a sharp XRPD pattern, indicating a retention of framework periodicity (compare Figure 6d,e). This pattern is not coincidental with that of the original unexchanged material; it appears to undergo lowering of symmetry to a periodic network that could not be determined with certainty. Nevertheless, upon addition of KNO_3(aq) to the exchanged solid, the transparency of the crystals is restored and their corresponding XRPD pattern is found to be indistinguishable from that of the original starting solid (compare parts d and f). The facility with which the ion exchange occurs coupled with the fact that the morphology of its crystalline particles is retained throughout the exchange process is further evidence that the anions are diffusing into the framework without any dissolution/recrystallization of the material or destruction of the host network.

Preventing Interpenetration. Examination of M−BPY frameworks (Figure 2) reveals that the rod-like BPY has a great tendency to form interpenetrated structures in the absence of either large guests or hydrogen-bonded and solvated ion guest aggregates. This is exemplified in the structure of $Ni(BPY)_{2.5}(H_2O)_2{\cdot}(BPY)_{1.5}(ClO_4)_2(H_2O)_2$, which is constructed from large square shaped building units of four $Ni(H_2O)_2^{2+}$ centers linked by BPY. Extension of these units in one dimension forms a porous cationic $Ni(BPY)_{2.5}(H_2O)_2^{2+}$ structure having railroad-like topology as schematically shown in Figure 2f.[12] Large pores of 11 × 11 Å dimension exist despite their tendency to interpenetrate; instead, the pores are found to be occupied by $(BPY)_{1.5}(ClO_4)_2(H_2O)_2$ guest aggregates. We believe that hydrogen-bonded guest aggregates such as those observed here prevent or reduce self-interpenetration by occupying the large voids in structures built from rod-like units. Additionally, due to their weak intermolecular interactions, their exchange is more facile than discrete guest ions.

Porous Frameworks Tailored for Highly Selective Separations

We have devoted considerable effort to developing synthetic strategies for designing porous networks with 1,3,5-benzenetricarboxylic acid (H_3BTC or BTC for the deprotonated form), where, in addition to size- and shape-selective binding, it would be possible to discriminate incoming molecules on the basis of their chemical affinity to the pores. The choice of BTC as a building block was motivated by its rigid disk-like conformation and its ability to bind metal ions in a multidentate fashion, which was expected to enhance the thermal stability and the structural rigidity of the resulting framework. Interpenetrated extended structures are less likely to form using BTC than BPY, due to the bulk associated with metal carboxylate aggregates.

Synthetic Strategies for Porous 1-D and 2-D Metal Carboxylate Frameworks. We have observed (Scheme 2) that, in the presence of competing ligands (L), BTC (triangles) binds to first-row transition metal ions within the same plane as either multi-bidentate, multi-monodentate, or a combination of both to give porous 1-D and 2-D metal carboxylate (M−BTC). The possibility exists of using a high M/BTC ratio with poorly ligating L to give zigzag chains, **d**, which are held together in the crystal by hydrogen bonds (dotted lines). Upon dissociation of L, guest molecules (filled circles) are introduced into the pores; thus, an open-framework material having accessible metal sites is achieved, **e**. This provides an opportunity for inclusion of guests with site-specific chemical selectiv-

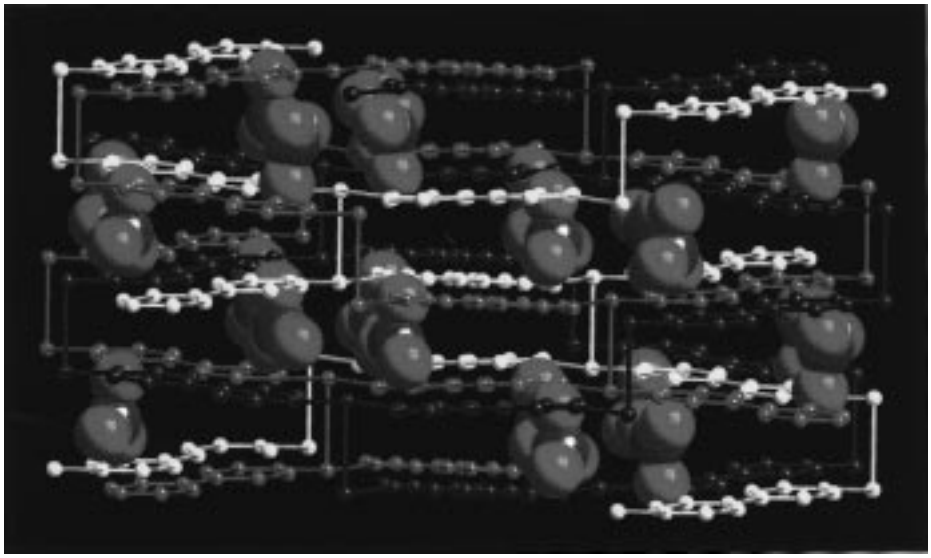

FIGURE 5. Crystal structure of Ag(BPY)•NO_3, where three interpenetrated networks (yellow, magenta, and green) result in rectangular pores that are occupied by nitrate anions (N, large blue; O, large red). The hydrogen atoms on BPY have been omitted for clarity.

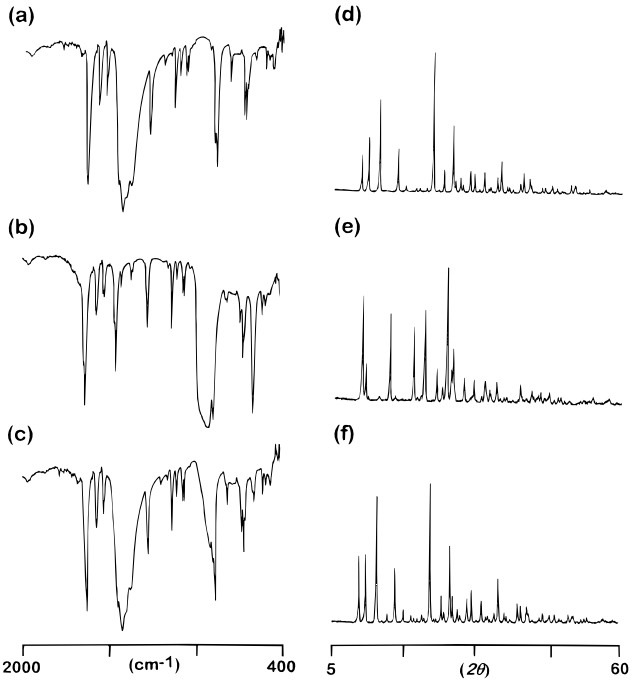

FIGURE 6. FT-IR spectra (a−c) and the corresponding X-ray diffraction patterns (d−f) showing the reversible anion exchange of PF_6^- for NO_3^- in Ag(BPY)•NO_3.

ity. On the other hand, when a low M/BTC ratio is used with a strong ligating L, alternating M−BTC and L layers are produced. Depending on the choice of L, a suitable environment capable of selective inclusion of guests between the M−BTC layers is created, **f**. In this way, on the basis of the ligating strength of L and the M/BTC ratio, it is possible to achieve porous 1-D and 2-D networks having pores with inclusion properties imparted by the choice of metal ion and molecular building block.

Porous Solids Assembled by Hydrogen-Bonded Chains. Following the synthetic strategy outlined in Scheme 2 for **d** and **e**, a series of compounds formulated as $M_3(BTC)_2$•-

Scheme 2

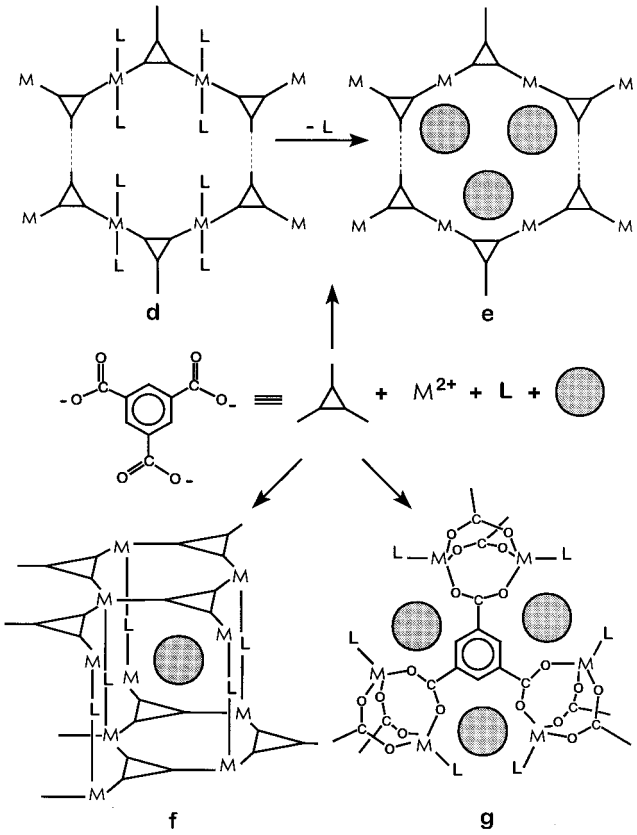

$12H_2O$ (M = Co, Ni, and Zn) were synthesized and structurally characterized. The hydrothermal reaction of metal(II) acetate hydrate with H_3BTC in an approximately 3/2 mole ratio at 140 °C yields red (Co), green (Ni), and colorless (Zn) crystals. These compounds are isostructural, as they show identical XRPD patterns. A single-crystal structure analysis performed on the $Co_3(BTC)_2$•-$12H_2O$ compound shows that the structure is composed of zigzag chains constructed from two symmetry-inequivalent tetraaquacobalt(II) units and BTC ligands as

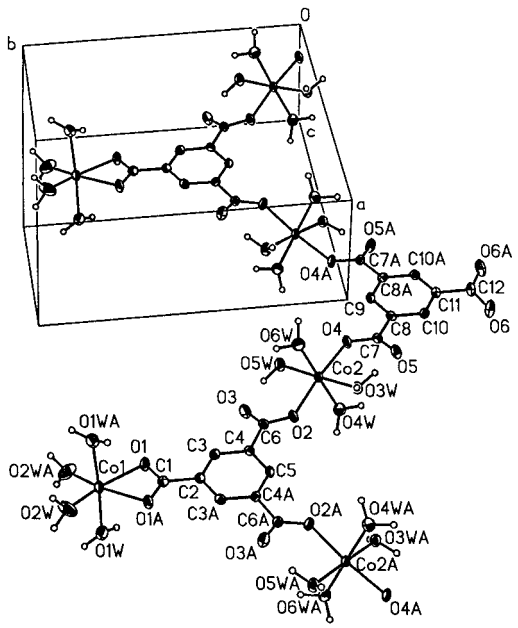

FIGURE 7. Co−BTC zigzag chain, including the asymmetric unit, present as the building block in crystalline $Co_3(BTC)_2{\cdot}12H_2O$. The non-hydrogen atoms are represented by thermal ellipsoids drawn at the 50% probability level. Atoms labeled with an additional letter A are symmetry equivalent to those atoms without such designation. The hydrogen atoms are drawn using an arbitrary sphere size for clarity.

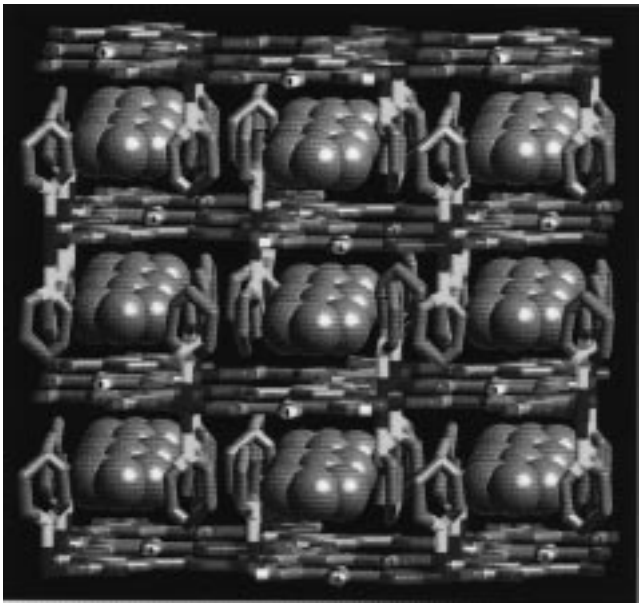

FIGURE 8. Crystal structure of $Co(HBTC)(NC_5H_5)_2{\cdot}(2/3)NC_5H_5$, showing the guest pyridine molecules (refined as benzene and drawn in space-filling gray spheres) occupying extended 1-D channels formed by Co−BTC−pyridine layers (shown as a cylinder representation with Co in green, O in red, N in yellow, and C in gray). All hydrogen atoms have been omitted for clarity.

shown in Figure 7.[13] Water ligands O3W and O5W on Co2 are engaged in hydrogen-bonding, respectively, to carboxylate oxygens O5 and O3 of an adjacent BTC within the chain, while O2W and O2WA on Co1 are hydrogen-bonded to O3W and O5W of an adjacent chain to form hydrogen-bonded layers. These layers are held together by similar but more numerous hydrogen-bonding interactions involving every remaining water and carboxylate unit in the structure to yield a tightly held 3-D solid having a total of 56 hydrogen-bonding interactions per formula unit (12/cobalt tetraaqua center and 10/BTC), which range from those considered strong, 2.554(4) Å, to those considered weak, 3.120(5) Å, hydrogen bonds.

Partial dehydration of this solid at 250 °C yields a porous $M_3(BTC)_2{\cdot}H_2O$ phase that is capable of reversible inclusion of water and ammonia. For the zinc compound, this process leaves no imprint on the framework, as no broadening of the XRPD peaks and no change in their intensity was observed compared to those of the fully hydrated starting material. The porous material is selective to water and ammonia, as no evidence for CO, CO_2, H_2S, CH_3CN, or C_5H_5N binding was observed. These results showed that it is possible to prepare porous materials that are based on 1-D metal−organic networks. Also, the selectivity of inclusion points to the possibility that the metal centers might be playing an important role in the binding of guests—an aspect that was pursued further for the synthesis of 3-D porous networks capable of highly selective inclusion of alcohols, vide infra.

Selective Adsorption of Aromatics. The strategy envisaged for **f** was realized by diffusing pyridine into an alcohol solution mixture of H_3BTC and $Co(NO_3)_2{\cdot}6H_2O$ to give large, pink, hexagonally shaped rod-like crystals $Co(HBTC)(NC_5H_5)_2{\cdot}(2/3)NC_5H_5$.[14] The structure of this compound is shown in Figure 8, where Co−BTC layers are found linked together only by strong $\pi-\pi$ interactions caused by the close proximity of pyridine ligands attached axially to the layers. The channels in this framework have a 7 × 7 Å cross-section, where free pyridine molecules reside. These channels can be evacuated at 200 °C to yield a stable porous network that is capable of removing the aromatic molecules from benzene/nitromethane, benzonitrile/acetonitrile, chlorobenzene/1,2-dichloromethane, and cyanobenzene/acetonitrile solution mixtures. This is very interesting since on the basis of their size and shape, all potential guests in these mixtures should be expected to permeate the pores. We believed that the observed selectivity toward benzene-containing guests is mainly due to their ability to π-stack between the BTC units within the sheets. Thus, the inclusion process is driven primarily by the electronic complementarity of the guests to the pores and not necessarily by their size or shape.

Tailoring Neutral 3-D Porous Frameworks for Site-Specific Binding. At this point it became clear to us that the dimensionality of the resulting M−BTC frameworks is mainly dependent on the M/BTC ratio and the ligating strength of L. However, consideration of an L that would only act to deprotonate H_3BTC without ligating to the metal led us to the synthesis of a 3-D porous system as shown in Scheme 2, **g**: It was postulated that a 3-D network, **g**, would be achieved upon employing a strong base such as triethylamine ($pK_a = 11.01$) with sufficient strength to completely deprotonate H_3BTC, but with poor affinity for binding to metal ions. Of course, the prevalent clustering of metal centers by BTC was expected since it

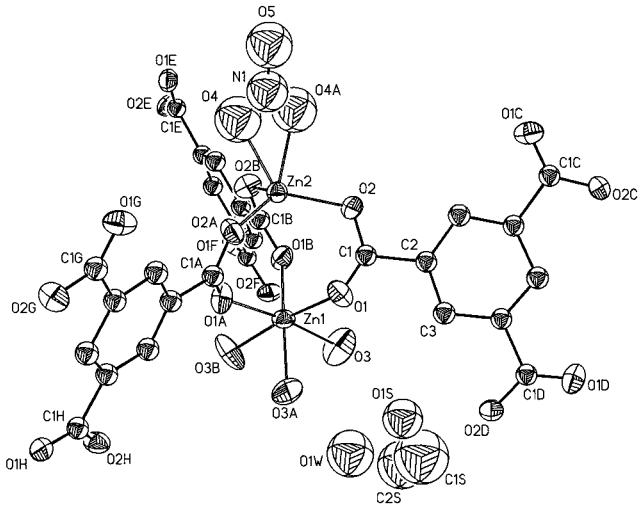

FIGURE 9. A perspective drawing of the building block unit for the structure of $Zn_2(BTC)(NO_3)\cdot(H_2O)(C_2H_5OH)_5$, with all the non-hydrogen atoms represented by 30% thermal ellipsoids. The coordinated nitrate anion is statistically disordered about the crystallographic 3-fold axis of the unit cell which passes through Zn1, Zn2, and O5; only one orientation for the nitrate anion is shown. All the hydrogen atoms have been omitted, and only the oxygen atoms (O3, O3A, and O3B) of the ethanol ligands are shown. Atoms labeled with additional subscripts A−H are symmetry related to atoms labeled without such subscripts.

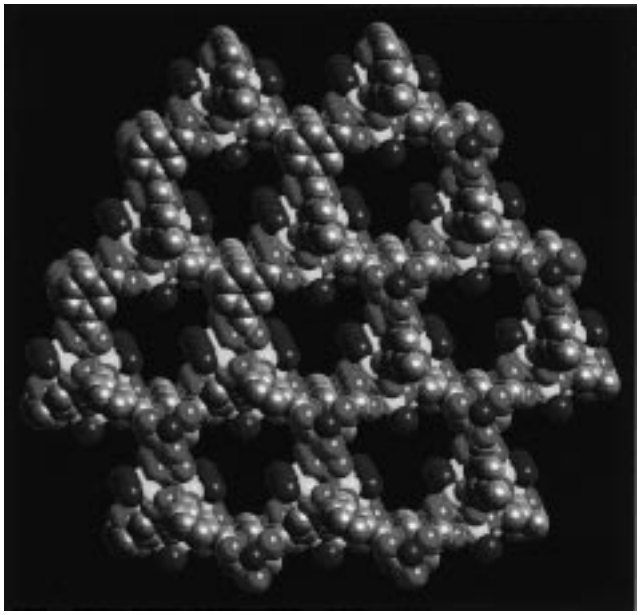

FIGURE 10. A space-filling representation of the 3-D structure of the $Zn_2(BTC)(NO_3)\cdot(H_2O)(C_2H_5OH)_5$ structure with C in gray, Zn in yellow, and O in red, with the green spheres, alternately, representing the nitrate anions and the three ethanol molecules as single spheres bound to Zn to emphasize the manner in which they point to the center of the cavity. All hydrogen atoms and ethanol/water guests have been omitted for clarity.

is a motif we often observe in this chemistry. The remaining site on the metal that is not occupied by the carboxylates of BTC will be available for binding a weak ligand L, in this case, either triethylamine or the solvent employed, which are weak ligands that can be evacuated to render the metal centers accessible to incoming ligands. In this way, a porous material is produced with its pores decorated by coordinately unsaturated metal centers as shown in **h**.

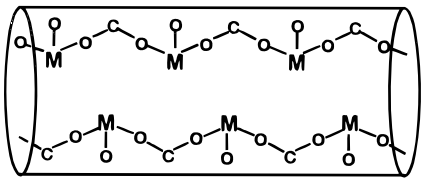

h

The success of this approach was demonstrated by the synthesis and structural characterization of a porous 3-D extended network having a rigid architecture which is held together by the multidentate functionalities of BTC. It was formulated as $Zn_2(BTC)(NO_3)\cdot(H_2O)(C_2H_5OH)_5$,[15] where the size, conformation, and triple-bidentate functionality of BTC enhance the rigidity of the Zn−BTC framework, thus allowing access to the metal centers through a 14 Å cross-section channel system that occupies a volume comprising nearly 44% of the structure. It is instructive to discuss the structure of this compound in some detail due to its relevance to the highly selective binding of guests.

The fundamental building unit of the crystal structure is shown in Figure 9. It is composed of two different zinc(II) centers (Zn1, Zn2) that are bridged by three carboxylates (O1, O2; O1A, O2A; O1B, O2B) of three separate BTC units, where all the symmetry-equivalent O1 atoms are linked to Zn1, and all the symmetry-equivalent O2 atoms are linked to Zn2. Progression of the structure in the crystal employs this unit and its linkage motif using the remaining carboxylate oxygens (O1C, O2C; O1E, O2E; O1H, O2H; and O1D, O2D; O1F, O2F; O1G, O2G) on each BTC unit. In this way, each BTC unit acts as a hexamonodentate unit, linking three pairs of zinc atoms to yield a tightly held framework, where each zinc atom has attained a trigonal pyramidal geometry with respect to its coordination to the BTC. The remaining positions on Zn1 and Zn2 are, respectively, occupied by three ethanol ligands (O3, O3A, O3B) and one bidentate nitrate (O4, O4A) ligand. The remaining ethanol (O1S, C1S, C2S) and water (O1W) molecules are isolated from and are not bound to the Zn−BTC building unit. The overall crystal structure of this material is shown in Figure 10. Here, the three ethanol and one nitrate ligands bound to Zn1 and Zn2 point toward the center of the channels, where the remaining two ethanol and one water molecule reside as guest inclusions. The nitrate ions are bound tightly to the zinc to give a Zn2−O4 distance of 2.14(6) Å, which does not allow for their ion exchange.

To access the channels, it would be imperative that at least unbound ethanol and water be removed since in their absence the diameter of the channels is expected to be approximately 9 Å with a free pore volume of 19.1% of the structure. Removal of the bound ethanol molecules would increase those values to 14 Å and 43.6%, respectively, and would allow the exploitation of the metal

reaction chemistry in connection to the feasibility of binding new guest molecules. Data obtained from a thermogravimetric study performed on a freshly prepared sample revealed that most bound and unbound ethanol can be removed from the channels at room temperature and atmospheric pressure prior to heating the sample. The mobility of ethanol within the channels has significant implications on the inclusion chemistry of this framework, as it renders easy access to zinc coordination sites within the channels. In fact, successful binding of small nonhindered alcohols such as methanol, ethanol, 1-propanol, 2-propanol, 1-butanol, and 2-methyl-2-propanol has been observed. No evidence was found for the binding of sterically hindered alcohols such as *tert*-butylphenol or nonalcoholic molecules such as chloroform, 1,2-dichloroethane, acetonitrile, nitrobenzene, cyanobenzene, toluene, acetone, and methyl ethyl ketone. It appears that the affinity toward nonsterically hindered alcohols is due to the precise demands of the zinc(II) coordination sites for alcohols, as other molecules of the proper size and shape but with different functional groups do not penetrate the channels.

The multidentate functionality of BTC and its ability to hold together a total of three pairs of zinc(II) centers lead to a rigid framework having unique stability toward inclusion. The aggregation of metal ion centers around BTC prevents interpenetration of the Zn−BTC porous network due to the bulk associated with such structural organization. Most significant is the tendency for ligands such as BTC to constrict the geometry around metal ions and yield accessible metal centers which is evident from our investigation of other networks based on the *cis*,*cis*-1,3,5-cyclohexanetricarboxylate (CTC) ligand, where its addition copolymerization with zinc(II) at 25 °C yields the extended coordination solid $Zn_3[(CTC)(C_5H_5N)]_2{\cdot}2(CH_3)_2NC(O)H$.[16] The metal carboxylate coordination pattern observed in the 2-D structure of this compound and the coordinative unsaturation on zinc are not dissimilar from those found in the aforementioned 3-D Zn−BTC framework.

Crystallization of Modular Solids

The greatest challenge to room-temperature synthesis of solid-state materials of the type discussed above is their attainment in a crystalline form amenable to single-crystal X-ray diffraction studies. In the course of studies we have observed that most of the simple procedures for crystal growth that are based on inducing crystallization by cooling, evaporation, or solvent diffusion are unsuitable for some of these materials. However, diffusion of a base in a metal−organic acid mixture as described above for BTC and the use of solvothermal techniques, when the building blocks have very poor solubility in a desirable solvent, have proved useful in obtaining materials with desirable crystallinity.[11−16]

We have also been using polymeric matrixes such as silicate and poly(ethylene oxide) gels to obtain single crystals from aqueous and nonaqueous reactions. It is one of the simplest, yet least utilized, methods of crystallization.[17] It is done by charging a gel with a known concentration of the chemical reagents needed in the synthesis, and then a solution containing the linking fragment is poured on top of the gel. A precipitate may form at the interface, but crystals of the assembled solid will form as the solution diffuses slowly through the gel. Often, the gel method is only employed to obtain specimens for X-ray single-crystal analysis, as the assembly in the absence of gel yields a pure microcrystalline phase of the material.[18]

Emerging Properties and Applications of Modular Porous Solids

The simple and high-yielding synthetic methods employed for the preparation of these materials are especially attractive for large-scale production. By using neutral building blocks such as BPY, it is possible to prepare porous cationic frameworks capable of reversible anion exchange—a process that was unknown in these systems at the outset of this work. Given that these materials are stable up to at least 230 °C, which exceeds the thermal stability of most anion-exchange resins, and their potential for affecting shape- and size-selective anion exchange, it is not unreasonable to anticipate their utility in the removal and recovery of inorganic and organic anions such as, MoO_4^{2-}, CN^-, HS^-, and $C_6H_5O^-$ from industrial wastewater.[19a−c]

The highly selective inclusion observed for the neutral networks that are based on BTC is extremely relevant to the removal and recovery of aromatics and halogenated hydrocarbons from industrial processes[19d−f] as illustrated by the chemistry of $Co(HBTC)(NC_5H_5)_2{\cdot}(2/3)NC_5H_5$. Our ability to synthesize accessible metal centers as represented by the chemistry of both $M_3(BTC)_2{\cdot}12H_2O$ and $Zn_2(BTC)(NO_3){\cdot}(H_2O)(C_2H_5OH)_5$ compounds provides opportunities for applications in air separation and liquid purification.[20,21] We anticipate that the ease with which such metal sites can be produced and functionalized will allow for the utility of these materials in low-temperature catalysis[2h,22] and in sensor development.[23]

Concluding Remarks

A new family of porous materials have been constructed from metal−organic and −inorganic cluster building blocks. By judicious choice of the building units, it is possible to produce extended anionic, cationic, and neutral porous networks with unusual pore architectures and functions. The building units, as well as the metal ions linking them, may be tailored to affect highly selective inclusion of incoming guests—a process that is apparently driven not only by the shape and size of guests, but also by their electronic and chemical affinity to the pores. Rigid porous frameworks have been produced which are capable of zeolite-like behavior, in that ion exchange and evacuation of the pores followed by readsorption of guests occur without destruction of the frameworks.

The great variety of starting materials that potentially can be used as building blocks in reactions similar to those

outlined here, coupled with the extensive knowledge of coordination chemistry available to synthetic chemists today, presents unparalleled opportunities for tailoring the topology and architecture of porous materials. We have herein outlined research that serves as an initial attempt at expressing design and rationality into materials synthesis. The emerging inclusion properties of these materials are examples of the far-reaching implications and significance of translating molecular chemistry into the solid state.

This work was supported by the National Science Foundation.

References

(1) See, e.g.: (a) Day, V. W.; Klemperer, W. G.; Mainz, V. V.; Millar, D. M. *J. Am. Chem. Soc.* **1985**, *107*, 8262. (b) Bautista, M. T.; White, P. S.; Schauer, C. K. *J. Am. Chem. Soc.* **1991**, *113*, 8963. (c) Cayton, R. H.; Chisholm, M. H.; Huffman, J. C.; Lobkovsky, E. B. *J. Am. Chem. Soc.* **1991**, *113*, 8709−8724. (d) Yaghi, O. M.; Sun, Z.; Richardson, D. A.; Groy, T. L. *J. Am. Chem. Soc.* **1994**, *116*, 807−808. (e) Hawthorne, M. F.; Zheng, Z. *Acc. Chem. Res.* **1997**, *30*, 267−276.

(2) See, e.g.: (a) Lu, J.; Paliwala, T.; Lim, S. C.; Yu, C.; Niu, T.; Jacobson, A. J. *Inorg. Chem.* **1997**, *36*, 923. (b) Losier, P.; Zaworotko, M. J. *Angew. Chem., Int. Ed. Engl.* **1996**, *35*, 2779. (c) Venkataraman, D.; Lee, S.; Moore, J. S.; Zhang, P.; Hirsch, K. A.; Gardner, G. B.; Covey, A. C.; Prentice, C. L. *Chem. Mater.* **1996**, *8*, 2030. (d) Yaghi, O. M. In *Access in Nanoporous Materials*; Pinnavaia, T. J., Thorpe, M. F., Eds.; Plenum: New York, 1995; p 111. (e) Robson, R.; Abrahams, B. F.; Batteen, S. R.; Gable, R. W.; Hoskins, B. F.; Liu, J. In *Supramolecular Architecture: Synthetic Control in Thin Films and Solids;* Bein, T., Ed.; American Chemical Society: Washington, DC, 1992; Chapter 19. (f) Iwamoto, T. In *Inclusion Compounds*; Atwood, J. L., Davies, J. E. D., MacNicol, D. D., Eds.; Oxford University Press: New York, Vol. 5, 177, 1991. (g) Hoskins, B. F.; Robson, R. *J. Am. Chem. Soc.* **1990**, *112*, 1546. (h) Fujita, M.; Kwon, Y. J.; Washizu, S.; Ogura, K. *J. Am. Chem. Soc.* **1994**, *116*, 1151. (i) Carlucci, L.; Ciani, G.; Proserpio, D. M.; Sironi, A. *J. Chem. Soc., Chem. Commun.*, **1994**, 2755. (j) Hoskins, B. F.; Robson, R.; Slizys, D. A. *J. Am. Chem. Soc.* **1997**, *119*, 2952−2953. (k) Gable, R. W.; Hoskins, B. F.; Robson, R. *J. Chem. Soc., Chem. Commun.* **1990**, 1677. (l) Kondo, M.; Yoshitomi, T.; Seki, K.; Matsuzaka, H.; Kitagawa, S. *Angew. Chem., Int. Ed. Engl.* **1997**, *36*, 1725.

(3) See, e.g. (a) MacGillivray, L. R.; Atwood, J. L. *Nature* **1997**, *389*, 469. (b) Russell, V. A.; Evans, C. C.; Li, W.; Ward, M. *Science* **1997**, *276*, 575. (c) Hollingsworth, M. D.; Brown, M. E.; Hillier, A. C.; Santarsiero, B. D.; Chaney, J. D. *Science* **1996**, *273*, 1355. (d) Garcia-Tellado, F.; Geib, S. J.; Goswami, S.; Hamilton, A. D. *J. Am. Chem. Soc.* **1991**, *113*, 9265−9269. (e) Etter, M. C. *Acc. Chem. Res.* **1990**, *23*, 120−126. (f) Seto, C. T.; Whitesides, G. M. *J. Am. Chem. Soc.* **1990**, *112*, 6409−6411. (g) Endo, K.; Sawaki, T.; Koyanagi, M.; Kobayashi, K.; Masuda, H.; Aoyama, Y. *J. Am. Chem. Soc.* **1995**, *117*, 8341−8352. (h) Wang, X.; Simard, M.; Wuest, J. D. *J. Am. Chem. Soc.* **1994**, *116*, 12119−12120. (i) Ermer, O.; Lindenberg, L. *Helv. Chim. Acta* **1991**, *74*, 825−877. (j) Copp, S. B.; Subramanian, S.; Zaworotko, M. J. *Angew. Chem., Int. Ed. Engl.* **1993**, *32*, 706−709.

(4) Michl, J., Ed. *Modular Chemistry*; Kluwer: Dordecht, The Netherlands, 1997.

(5) Wells, A. F. *Structural Inorganic Chemistry*; Oxford University Press: Oxford, 1984.

(6) O'Keeffe, M.; Hyde, B. G. *Crystal Structures*; Mineralogical Society of America: Washington, DC, 1996.

(7) Yaghi, O. M.; Richardson, D. A.; Li, G.; Davis, C. E.; Groy, T. L. *Mater. Res. Soc. Symp. Proc.* **1995**, *371*, 15−19.

(8) (a) Bedard, R. L., Wilson, S. T., Vail, L. D., Bennett, J. M., Flanigen, E. M., Jacobs, P. A., van Santen, R. A., Eds. *Zeolites: Facts, Figures, Future*; Elsevier: Amsterdam, The Netherlands, 1989. (b) Dhingra, S.; Kanatzidis, M. G. *Science* **1992**, *258*, 1769−1772. (c) Parise, J. B. *Science* **1991**, *251*, 293−294. (d) Dance, I. G.; Garbutt, R. G.; Craig, D. C.; Scudder, M. L. *Inorg. Chem.* **1987**, *26*, 4057−4064. (e) Bowes, C. L.; Ozin, G. A. *Adv. Mater.* **1996**, *8*, 13.

(9) (a) MacGillivray, L. R.; Subramanian, S.; Zaworotko, M. J. *J. Chem. Soc., Chem. Commun.* **1994**, 1325. (b) Carlucci, L.; Ciani, G.; Proserpio, D. M.; Sironi, A. *J. Chem. Soc., Chem. Commun.* **1994**, 2755.

(10) (a) Yaghi, O. M.; Li, H. *J. Am. Chem. Soc.* **1995**, *117*, 10401−10402. (b) Yaghi, O. M.; Li, H. *J. Am. Chem. Soc.* **1996**, *118*, 295−296.

(11) Yaghi, O. M.; Li, G. *Angew. Chem., Int. Ed. Engl.* **1995**, *34*, 207.

(12) Yaghi, O. M.; Li, H.; Groy, T. L. *Inorg. Chem.* **1997**, *36*, 4292−4293.

(13) Yaghi, O. M.; Li, H.; Groy, T. L. *J. Am. Chem. Soc.* **1996**, *118*, 9096−9101.

(14) Yaghi, O. M.; Li, G.; Li, H. *Nature* **1995**, *378*, 703−706.

(15) Yaghi, O. M.; Davis, C. E.; Li, G.; Li, H. *J. Am. Chem. Soc.* **1997**, *119*, 2861−2868.

(16) Yaghi, O. M.; Jernigan, R.; Li, H.; Davis, C. E.; Groy, T. L. *J. Chem. Soc., Dalton Trans.* **1997**, 2383−2384.

(17) (a) Henisch, H. K. *Crystal Growth in Gels*; Pennsylvania State University Press: University Park, PA, 1970. (b) Henisch, H. K. *Crystals in Gels and Liesegang Rings*; Cambridge University Press: Cambridge, 1988. (c) McCauley, J. W.; Roy, R. *Am. Mineral.* **1974**, *59*, 947. (d) Holmes, H. N. *J. Franklin Inst.* **1917**, *184*, 743. (e) Cody, A. M.; Horner, H. T.; Cody, R. D. In *Scanning Electron Microscopy*; Johari, O., Albrecht, R. M., Eds.; Scanning Microscopy: Chicago, 1982. (f) Holmes, H. N. In *Colloid Chemistry*; Alexander, J., Ed.; Chemical Catalog Co.: New York, 1926. (g) Suib, S. L. *J. Chem. Educ.* **1985**, *62*, 81.

(18) Crystallization methods involving the aqueous (a) and nonaqueous (b) gel method have been employed for the achievement of porous modular solids in the form of single crystals: (a) Yaghi, O. M.; Li, G.; Groy, T. L. *J. Solid State Chem.* **1995**, *117*, 256. (b) Yaghi, O. M.; Li, G.; Li, H. *Mater. Chem.* **1997**, *9*, 1074.

(19) (a) Eilbeck, W. J.; Mattock, G. *Chemical Process in Wastewater Treatment*; John Wiley and Sons: New York, 1987. (b) Abdo, M. S. E.; Nosier, S. A.; El-Khaiary, M. I. *J. Environ. Sci. Health* **1997**, *32*, 1159. (c) Heininger, M. W.; Meloan, C. E. *Sep. Sci. Technol.* **1992**, *27*, 663. (d) Lanouette, K. H. *Chem. Eng.* **1977**, *84*, 99−106. (e) Glynn, W., Baker, C., LoRe, A., Quaglieri, A., Eds. *Mobil Waste Processing Systems and Treatment Technologies*; Noyes Data Co.: NJ; 1987. (f) Collie, M. J. *Industrial Water Treatment Chemicals and Processes*; Noyes Data Co.: NJ, 1983.

(20) Ramprasad, D.; Pez, G. P.; Toby, B. H.; Markley, T. J.; Pearlstein, R. M. *J. Am. Chem. Soc.* **1995**, *117*, 10694−10701.
(21) Yaghi, O. M., *Crystalline Metal-Organic Microporous Materials.* US Patent No. 5, 648,508, 1997.
(22) Reis, K. P.; Joshi, V. K.; Thompson, M. E. *J. Catal.* **1996**, *161*, 62−67.
(23) (a) Zhu, S. S.; Carroll, P. J.; Swager, T. M. *J. Am. Chem. Soc.* **1996**, *118*, 8713−8714. (b) Brousseau, L. C.; Mallouk, T. E. *Anal. Chem.* **1997**, *69*, 679.

AR970151F